Structural Changes of Surface Layer of Vanadyl Pyrophosphate Catalysts by Oxidation−Reduction and Their Relationships with Selective Oxidation of *n*-Butane

Gaku Koyano, Toshio Okuhara,† and Makoto Misono*

Contribution from the Department of Applied Chemistry, Graduate School of Engineering, The University of Tokyo, Bunkyo-ku, Tokyo 113, Japan

Received December 27, 1996

Abstract: The surface structure of vanadyl pyrophosphate ($(VO)_2P_2O_7$) and its changes upon controlled oxidation and reduction have been investigated comprehensively by means of Raman spectroscopy, X-ray photoelectron spectroscopy (XPS), thermogravimetry (TG), EXAFS, X-ray diffraction (XRD), transmission electron diffraction (TED), and "micropulse" reaction of *n*-butane. Oxidation of a well-defined $(VO)_2P_2O_7$ with O_2 (1 atm) at 733 K formed "X_1 phase" as a thin surface overlayer on $(VO)_2P_2O_7$, where X_1 phase is a phase reported previously (Shimoda, T.; Okuhara, T.; Misono, M. *Bull. Chem. Soc. Jpn*. **1985**, *58*, 2163−2171) and similar to δ-$VOPO_4$. By the repeated micropulse reactions of *n*-butane, the surface X_1 phase was gradually reduced back to $(VO)_2P_2O_7$, showing that reversible redox reactions between X_1 phase and $(VO)_2P_2O_7$ occur by the reactions with butane and oxygen. XRD, EXAFS, and TED demonstrated that X_1 phase has a structure analogous to $(VO)_2P_2O_7$, in both of which V−O−V pair sites exist. The micropulse reaction of *n*-butane with the surface X_1 phase produced maleic anhydride with a significantly higher selectivity (∼40%) than that with β-$VOPO_4$ (<10%). These results indicate that X_1 phase is the real active phase involved in the redox cycle for the oxidation of *n*-butane to maleic anhydride over $(VO)_2P_2O_7$.

Introduction

It is generally accepted that $(VO)_2P_2O_7$ has a characteristic function for selective catalytic oxidation of *n*-butane to maleic anhydride (abbreviated as MA) and that this is the main component of industrial catalysts for this reaction.[1−3] No other mixed oxides show performance comparable with $(VO)_2P_2O_7$. However, the real active component of this catalyst system has been controversial for many years. Some researchers have proposed that the single crystalline phase of $(VO)_2P_2O_7$ itself is the active phase for this reaction.[4−6] Bordes et al.[7] and Volta et al.[8] have indicated that a biphasic catalyst consisting of $(VO)_2P_2O_7$ and γ-$VOPO_4$ is active. On the contrary, Yamazoe et al.[9] and Hutchings et al.[10] inferred that a phosphorus-rich phase (P/V ∼2) on the surface of $(VO)_2P_2O_7$ is important for this reaction. Besides, it has been claimed that a special activation treatment in a flow of reactant is indispensable to obtain high catalytic performance.[11]

To elucidate the mechanism, the oxidation−reduction processes of the surface of $(VO)_2P_2O_7$ are of great concern, as a Mars van Krevelen mechanism[12] is considered to be involved in the selective oxidation of *n*-butane to MA.[13] It has frequently been suggested that the redox between V^{4+} and V^{5+} phase operates in this reaction.[8,13−15] On the other hand, Trifiro et al.[1,16] indicated from UV spectroscopy that a redox cycle between V^{3+} and V^{4+} is responsible for the selective oxidation. Recently, Gai et al.[17] presumed that V^{3+} species, which are located next to the oxygen defect sites, play important roles in selective oxidation of *n*-butane.

As for the behavior of oxygen, Pepera et al.[13] reported that the isotopic oxygen exchange between the surface layer of $(VO)_2P_2O_7$ and the gas phase took place rapidly, but that between the surface and bulk was slow. The authors' group[14] also showed by an isotopic study that the diffusion of oxygen atoms is limited to a few surface layers of $(VO)_2P_2O_7$ during the oxidation of *n*-butane.

* Author to whom correspondence should be addressed. Tel: +81−3−3812−2111 (ext 7272). Fax: +81-3-5802-2949. E-mail: tmisono@hongo.ecc.u-tokyo.ac.jp.

† Present address: Graduate School of Environmental Earth Science, Hokkaido University, Sapporo 060, Japan. Tel: +81-11-706-5280. Fax: +81-11-757-5995. E-mail: oku@ees.hokudai.ac.jp.

(1) Centi, G.; Trifiro, F.; Ebner, J. R.; Franchetti, V. M. *Chem. Rev.* **1988**, *88*, 55.
(2) Hodnett, B. K. *Catal. Rev. − Sci. Eng*. **1985**, *27*, 373.
(3) Centi, G. *Catal. Today* **1993**, *16*, 5.
(4) Shimoda, T.; Okuhara, T.; Misono, M. *Bull. Chem. Soc. Jpn*. **1985**, *58*, 2163.
(5) Moser, T. P.; Schrader, G. L. *J. Catal.* **1985**, *92*, 216.
(6) Busca, G.; Cavern, F.; Centi, G.; Trifiro, F. *J. Catal*. **1986**, *99*, 400. Yang, T. C.; Rao, K. K.; Der Huang, I. US Patent 4,392,986, 1987.
(7) Bordes, E. *Catal. Today*, **1987**, *1*, 499.
(8) (a) Abdelouahab, F. B.; Olier, R.; Guilhaume, N.; Lefebvre, F.; Volta, J. C. *J. Catal*. **1992**, *134*, 151, (b) Hutchings, G. H.; Chomel, A. D.; Olier, R.; Volta, J. C. *Nature* **1994**, *368*, 41.
(9) Morishige, H.; Tamaki, J.; Miura, N.; Yamazoe, N. *Chem. Lett*. **1990**, 1513.
(10) (a) Sananes, M. T.; Hutchings, G. J.; Volta, J. C. *J. Chem. Soc., Chem. Commun*. **1995**, 243, (b) Sananes, M. T.; Hutchings, G. J.; Volta, J. C. *J. Catal*. **1995**, *154*, 253−260.
(11) For example: Albonetti, S.; Cavani, F.; Trifiro, F.; Venturoli, P.; Calestani, G.; Granados, M. L.; Fierro, J. L. G. *J. Catal*. **1996**, *160*, 52.
(12) Mars, P.; van Krevelen, D. W. *Chem. Eng. Sci*. **1954**, *3*, 41.
(13) Pepera, M.; Callahan, J. L.; Desmond, M. J.; Milberger, E. C.; Blum, P. R.; Bremer, N. J. *J. Am. Chem. Soc*. **1985**, *107*, 4883.
(14) Misono, M.; Miyamoto, K.; Tsuji, K.; Goto, T.; Mizuno, N.; Okuhara, T. In *Studies in Surface Science and Catalysis, Vol. 82, New Developments in Selective Oxidation*; Centi, G.; Trifiro, F., Eds.; Elsevier: Amsterdam, 1990; p 605.
(15) Koyano, G.; Okuhara, T.; Misono, M. *Catal. Lett*. **1995**, *32*, 205.
(16) Cavani, F.; Trifiro, F. *Chemtech* **1994**, *24*, 18.
(17) Gai, L. P.; Kourtakis, K. *Science* **1995**, *267*, 661.

S0002-7863(96)04437-X CCC: $15.00 © 1998 American Chemical Society
Published on Web 01/17/1998

Therefore, for the understanding of the unique catalysis of $(VO)_2P_2O_7$ in the selective oxidation of *n*-butane to MA, the elucidation of the structural changes of the surface of $(VO)_2P_2O_7$ upon redox treatment is the most critical subject. Besides $(VO)_2P_2O_7$, there are several V−P−O phases having P/V = 1. Their catalytic features may also be informative. As for V^{5+} phases, β-$VOPO_4$,[18] α-$VOPO_4$,[19] X_1 phase,[4] X_2 phase,[4] γ-$VOPO_4$,[20] δ-$VOPO_4$,[20] β' phase,[21] and β'' phase[21] have been reported. X_1 and β'' phases are most probably identical, since the X-ray diffraction (XRD) patterns agreed.[4,21] δ-$VOPO_4$ shows the same Raman spectrum[8,15] and a similar XRD pattern[4,20] as the X_1 phase; these two phases are considered to have similar structures. Each phase showed different activity and selectivity for *n*-butane oxidation;[4,22] e.g., α- and β-$VOPO_4$ were much less selective than X_1 phase, γ-$VOPO_4$, and $(VO)_2P_2O_7$. Here, it must be reminded that the structure sometimes changes by the reaction.

Structures of β-$VOPO_4$,[18] α-$VOPO_4$,[19] and $(VO)_2P_2O_7$[23] were determined by single-crystal X-ray diffraction. VO_6 octahedra are isolated in α- and β-$VOPO_4$, while an edge-sharing structure of two VO_6 units (pair sites) is present in $(VO)_2P_2O_7$. But the structures of X_1 phase (similar to δ-$VOPO_4$) and γ-$VOPO_4$ remained unsolved. Volta et al.[8,24] deduced by Raman spectroscopy and solid-state NMR that γ- and δ-$VOPO_4$ do not contain V−O−V pair sites. On the other hand, Matsuura[21] proposed on the basis of the powder XRD pattern that β" phase contains V−O−V pair sites. The authors[25] suggested from the results of EXAFS that the V−O−V pair sites are present in the structure of X_1 phase.

Raman spectroscopy is proven to be useful for the analysis of the structural changes of VPO phases with the reaction.[8,15,26] Schrader et al. examined the oxidation process of $(VO)_2P_2O_7$ to β-$VOPO_4$ with $^{18}O_2$.[26] Volta and co-workers[8] suggested that γ-$VOPO_4$ formed on the surface of $(VO)_2P_2O_7$ is active for the selective oxidation.

In the present study, the changes of the surface structure of $(VO)_2P_2O_7$ upon oxidation and reduction have been investigated by means of various spectroscopic methods and micropulse reaction of *n*-butane and/or oxygen. X_1 phase, a plausible V^{5+} phase involved in the redox process, was characterized by XPS, EXAFS, and TED. The redox processes during the catalytic oxidation of *n*-butane over $(VO)_2P_2O_7$ are discussed in relation to these structural changes of the surface of $(VO)_2P_2O_7$.

Experimental Section

Preparation of $(VO)_2P_2O_7$. Two kinds of a precursor, vanadium hydrogen phosphate hemihydrate ($VOHPO_4 \cdot 0.5H_2O$), P-3 and P-4, were prepared as reported previously.[27] P-3 was obtained from the so-called organic solvent method as follows. V_2O_5 (0.08 mol) was added to a mixture of isobutyl alcohol (90 mL) and benzyl alcohol (60 mL), and the suspension was then refluxed at 378 K for 3 h. After the suspension was cooled to room temperature, an aqueous solution of H_3PO_4 (85% H_3PO_4, 0.16 mol) was added to the suspension and was again refluxed at 378 K for 3 h. The resulting greenish light blue solid was filtered off, washed with acetone, and dried at room temperature. The XRD pattern of this solid was in agreement with that of $VOHPO_4 \cdot 0.5H_2O$.[28]

P-4 was obtained by reduction of $VOPO_4 \cdot 2H_2O$ with 2-butanol under reflux. $VOPO_4 \cdot 2H_2O$ was first prepared as follows: V_2O_5 powder (0.15 mol) was added to 250 g of the aqueous solution of 85% H_3PO_4 (H_3PO_4, 2.2 mol). The resulting yellow solution was refluxed at 348 K for 24 h. The solid obtained was filtered off and washed with water for several times. The solid gave the same XRD pattern as $VOPO_4 \cdot 2H_2O$.[29] The $VOPO_4 \cdot 2H_2O$ (14 g) obtained was reduced with 2-butanol (150 mL) at 363 K for 18 h to form P-4.

Vanadyl pyrophosphate catalysts ($(VO)_2P_2O_7$) were obtained from P-3 and P-4 as follows. These precursors were treated at 823 K in an N_2 flow for 5 h, and then calcined in a flow of air (90 mL·min^{-1}) at 733 K for 0.5 h (P-3) and 2 h (P-4). Then these were dispersed into water. The slurries were stirred for 3 h at room temperature, and the solids were filtered and washed with water. The obtained solids (catalysts) are denoted by C-3 and C-4, respectively.

Preparation of Various $VOPO_4$. X_1 phase was synthesized from NH_4HVPO_6 as described previously.[4] An aqueous solution of $NH_4H_2PO_4$ ($NH_4H_2PO_4$, 0.8 mol; H_2O, 600 mL) containing V_2O_5 powder (0.04 mol) was boiled for 0.5 h and then cooled to room temperature to obtain the precipitate of NH_4HVPO_6. After filtration, the solid was treated in an O_2 flow at 823 K for 5 h. The resulting solid was confirmed to be X_1 phase by XRD.[4] The surface area was 28 m^2·g^{-1}.

β-$VOPO_4$ was prepared by calcination of $VOHPO_4 \cdot 0.5H_2O$, which was obtained by adding V_2O_5 powder (0.1 mol) and H_3PO_4 (0.2 mol) into an aqueous solution of $NH_2OH \cdot HCl$ (0.2 mol in 200 mL) at 873 K in the O_2 flow for 10 h as reported previously.[4] The surface area was 3.2 m^2·g^{-1}. The XRD pattern of the solid was in good agreement with that in the literature.[4]

Calcination of $(NH_4)_2[(VO)_2C_2O_4(HPO_4)_2]$ in an O_2 flow at 873 K for 10 h produced α-$VOPO_4$, where $(NH_4)_2[(VO)_2C_2O_4(HPO_4)_2]$ was prepared from an aqueous solution of oxalic acid (0.30 mol in 400 mL) by adding V_2O_5 powder (0.1 mol) and $NH_4H_2PO_4$ (0.2 mol).[4] The surface area was 5.9 m^2·g^{-1}. The XRD pattern of the solid was in good agreement with that in the literature.[4]

Oxidation of $(VO)_2P_2O_7$ with O_2. Oxygen treatment was performed with O_2 (1 atm, 60 mL·min^{-1}) in the range from 733 to 823 K after $(VO)_2P_2O_7$ was treated in a flow of He (1 atm, 60 mL·min^{-1}) at 773 K for 1 h. The degree of the oxidation state was controlled by the temperature and time period. Uptakes of oxygen were monitored by the weight increase, which were measured by a microbalance (Seiko Instruments, TG/DTA 220), in which the sample (∼6 mg) was set in a Pt pan. The oxidation state is expressed in the following two ways: x in $V^{4+}{}_{1-2x}V^{5+}{}_{2x}PO_{4.5+x}$ (=$VPO_{4.5+x}$) and the number of V^{5+} layers (abbreviated as NL), where the latter for NL < 1 is the ratio of the number of V^{5+} to the number of vanadium atoms (V^{4+} + V^{5+}) in the surface monolayer of $(VO)_2P_2O_7$. The number of vanadium atoms in the surface monolayer was estimated to be 8.1×10^{-4} and 1.3×10^{-4} mol·g^{-1} for C-3 and C-4, respectively, from the surface area and the surface concentration of V atoms on the (100) plane.[23]

Characterization of Catalysts. Raman spectra were recorded with a Laser Raman spectrometer (Jasco Corp., NR-1800) using the 514.5 nm line from an Ar ion laser (NEC GLS3261J). Sample powder was put on a glass sample holder. The power of the laser was usually set below 20 mW to avoid the destruction of the samples. Raman sensitivities for X_1 phase and $(VO)_2P_2O_7$ were determined by macroscopic measurement of physical mixtures of $(VO)_2P_2O_7$ (C-3) and X_1 phase having different ratios. It was observed that the sensitivity of X_1 phase was about 10 times higher than that of $(VO)_2P_2O_7$.

X-ray photoelectron spectroscopy (XPS) spectra were recorded with a JEOL JPS-90-SX spectrometer with Al Kα radiation. The sample was pressed into a self-supporting disk and evacuated in the chamber at room temperature for 12 h to remove water on the sample. To avoid the reduction of the sample during the measurement by X-ray, the

(18) Gopal, R.; Calvo, C. *J. Solid State Chem.* **1972**, *5*, 432.
(19) Jordan, B.; Calvo, C. *Can. J. Chem.* **1972**, *51*, 2621.
(20) Bordes, E.; Courtine, P. *J. Chem. Soc., Chem. Commun.* **1985**, 294.
(21) Matsuura, I.; Mori, A.; Yamazaki, M. *Chem. Lett.* **1987**, 1897.
(22) Lin, Y. Z.; Forissier, M.; Sneeden, R. P.; Vedrine, J. C.; Volta, J. C. *J. Catal.* **1994**, *145*, 256.
(23) Gorbunova, Y. E.; Linde, S. A. *Sov. Phys. Dokl.* **1979**, *24*, 138.
(24) Abdelouahab, F. B.; Volta, J. C.; Olier, R. *J. Catal.* **1994**, *48*, 334.
(25) Koyano, G.; Yamaguchi, F.; Okuhara, T.; Misono, M. *Shokubai* **1995**, *37*, 80.
(26) Moser, T. P.; Schrader, G. L. *J. Catal.* **1991**, *128*, 113.
(27) Igarashi, H.; Tsuji, K.; Okuhara, T.; Misono, M. *J. Phys. Chem.* **1993**, *97*, 7065.
(28) Johnson, J. W.; Johnston, D. C.; Jacobson, A. J.; Brody, J. F. *J. Am. Chem Soc.* **1984**, *106*, 8123−8128.
(29) R'kha, C.; Vandenborre, M. T.; Livage, J. *J. Solid State Chem.* **1986**, *63*, 202−215.

spectra of oxidized $(VO)_2P_2O_7$ were taken in only one accumulation. The binding energy was referenced to the O_{1s} binding energy of 532.0 eV.

The shape and size of the particles of $(VO)_2P_2O_7$ (C-3 and C-4) were measured by scanning electron microscopy (SEM; JEOL TSM-T20). The samples were suspended in acetone and dispersed on a covering glass. After the samples were dried at room temperature, Au was deposited on them.

X-ray diffraction (XRD) patterns were measured with an X-ray diffractometer (MAC Science MXP^3) using Cu Kα radiation (λ = 1.5405). EXAFS was measured at National Laboratory for High Energy Physics, Photon Factory (BL-7C) at 80 K. The sample (10−45 mg) was mixed with a cellulose powder as a binder and pressed (100 kgf·cm^{-2}) into disks (10 mm diameter) in dry air. All data were analyzed with the same method as described elsewhere.[30,31]

Transmission electron diffraction (TED) was measured with a JEOL JEM-4000FX II electron microscope with an acceleration voltage of 400 kV. The bulk X_1 phase used for the TED measurement was prepared from plate-like $(VO)_2P_2O_7$ (C-4) by the oxidation at 823 K for 5 h.

Surface area of the catalyst was measured by the BET method using N_2 with Micromeritics ASAP-2000, after the samples were treated in a vacuum at 573 K for 1 h.

Micropulse Reaction. A micropulse reaction was performed in the pulsereactor (Pyrex, 10 mm in diameter) connected with a flow system. At the outlet of the reactor, a quadrupole mass spectrometer (Anelva AGA-100; acceleration, 30 eV) was directly connected. After the catalyst was treated in He (60 mL·min^{-1}) at 773 K for 1 h, it was calcined in an O_2 flow for 2 h at 733 K. The pulse of *n*-butane (0.71 mL of 2.0% *n*-butane in He; *n*-butane = 6.0×10^{-7} mol) was injected into the He flow repeatedly at intervals of about 1 min. The flow rate was precisely controlled by thermal mass flow controllers (Ueshima-Brooks 5800). A mass spectrometer was connected to a microcomputer to collect the data in the range m/z = 26−60 at every 0.3 s. The composition of MA at the outlet was estimated using the peak intensity of m/z 54 after the subtraction of the contributions of fragmentation of *n*-butane, butene, and butadiene. The compositions of *n*-butane, butenes, butadiene, furan, CO, and CO_2 were also calculated from the relative peak intensities of m/z 28, 39, 41, 43, 44, 54, and 68. Sensitivity factors of these gases for the mass spectrometric analysis were directly determined by using each gas.

Catalytic Reaction. Catalytic oxidation of *n*-butane was carried out in a conventional flow reactor made of Pyrex tubing (inside diameter 10 mm). A mixture of 1.5% *n*-butane and 17% O_2 (N_2 balance) was passed (20 mL·min^{-1}) over the catalyst bed (200 mg) at 733 K. Since nearly stationary state was obtained after 2 h, the conversion and selectivity were measured at 5 h.

Results

The structures of the two $(VO)_2P_2O_7$ samples, C-3 and C-4, were confirmed by XRD to be identical with those reported previously.[27] Surface P/V ratios of C-3 and C-4 were about 1.1, which was estimated from the XPS peak intensity according to the method described previously by the authors.[32] The main difference between C-3 and C-4 is the shape of the crystallites and hence the BET surface area. C-3 and C-4 have rose-petal-like and plate-like hexagon structures, respectively.[27] The width of the hexagons determined by SEM micrograph were 1 μm × 1 μm and 5 μm × 5 μm for C-3 and C-4, respectively.[27] The thickness of the crystallites estimated from the XRD line width were 8 and 40 nm for C-3 and C-4, respectively.[27] BET surface areas of C-3 and C-4 were 78 and 13 m^2·g^{-1}, respectively. The $(VO)_2P_2O_7$ used for the pulse reaction, Raman spectroscopy, and XPS was C-3, because of its larger surface area. C-4 was applied to TED analysis for the reason of crystallinity.

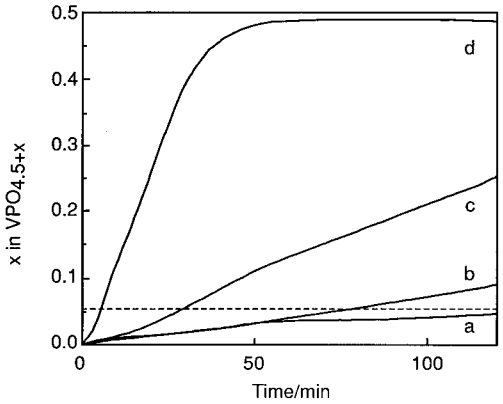

Figure 1. Time courses of O_2 uptake for $(VO)_2P_2O_7$ (C-3). Flow rate of O_2: 100 mL·min^{-1}, 1 atm. The oxidation state, x (in the ordinate), was calculated from the weight increase by O_2 uptake. Oxidation temperature: (a) 733 K, (b) 753 K, (c) 773 K, and (d) 823 K. Dotted line corresponds to the monolayer oxidation.

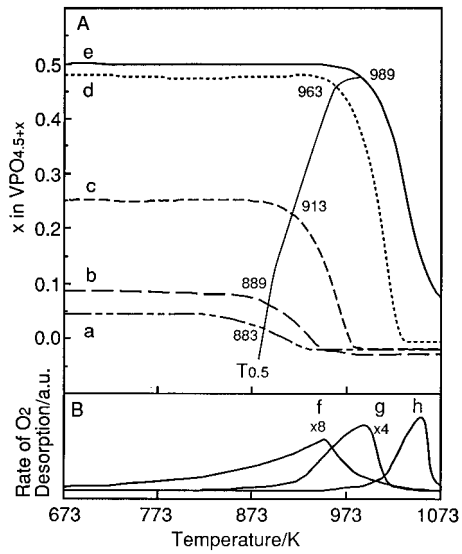

Figure 2. Temperature-programmed desorption (TPD) of O_2 monitored by weight loss with a microbalance (A) and rate of O_2 desorption (B). Prior to the TPD, $(VO)_2P_2O_7$ (C-3) was oxidized at (a) 733 K, (b) 753 K, (c) 773 K, (d) 823 K, (f) 733 K, and (g) 773 K for 2 h. (e) and (h) show the results of β-$VOPO_4$. Flow rate of He was 100 mL·min^{-1}. $T_{0.5}$ shows the temperature at which the amounts of desorbed oxygen correspond to a half monolayer (NL = 0.5).

Figure 1 shows the time courses of oxygen uptake measured by the microbalance for $(VO)_2P_2O_7$ (C-3) at elevated temperatures. Prior to the supply of the O_2 flow, the sample was pretreated in the He flow at 733 K for 1 h. The value of x (x in $VPO_{4.5+x}$ as defined in the Experimental Section) corresponding to monolayer oxidation is shown by a broken line in Figure 1. The uptake of O_2 was slow at 733 K; the oxidation was less than the surface monolayer after 2 h (a in Figure 1). At 753 and 773 K, the degrees of the oxidation after 2 h were x = 0.080 (NL = 1.6) and x = 0.25 (NL = 4.9), respectively. At 823 K, nearly the whole bulk was oxidized to form $VOPO_4$ in 50 min, the oxygen uptake nearly corresponding to $V^{4+} \rightarrow V^{5+}$.

Figure 2 provides the temperature-programmed desorption of O_2 from the oxidized $(VO)_2P_2O_7$ (C-3) and β-$VOPO_4$. The weight decrease measured by the microbalance and the rate of the O_2 desorption determined by a mass spectrometer are shown in A and B of Figure 2. As shown in a−d in Figure 2A, oxygen atoms held by the catalyst were desorbed up to 1030 K. The

(30) Miyanaga, T.; Fujikawa, T.; Matsubayashi, N.; Fukumoto, T.; Yokoi, K.; Watanabe, I.; Ikeda, *S. Bull. Chem. Soc. Jpn.* **1989**, *62*, 1791.
(31) Matsubayashi, N. Thesis, Osaka University, 1986.
(32) Okuhara, T.; Nakama, T.; Misono, M. *Chem. Lett.* **1990**, 1941.

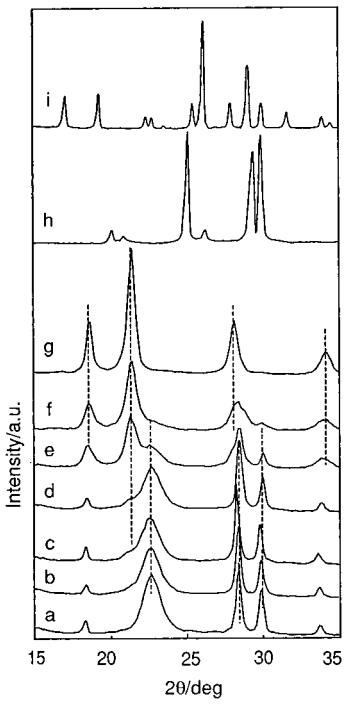

Figure 3. Changes in the XRD pattern upon oxidation. $(VO)_2P_2O_7$ (C-3) was treated in an O_2 flow (60 mL·min^{-1}, 1 atm) for 2 h at (a) 300 K ($x = 0$, NL = 0), (b) 713 K ($x = 0.011$, NL = 0.21), (c) 733 K ($x = 0.047$, NL = 0.94), (d) 753 K ($x = 0.080$, NL = 1.6), (e) 773 K ($x = 0.25$, NL = 4.9), and (f) 823 K ($x = 0.48$, NL = 9.6). XRD patterns of $VOPO_4$; (g) X_1 phase, (h) α-$VOPO_4$, and (i) β-$VOPO_4$.

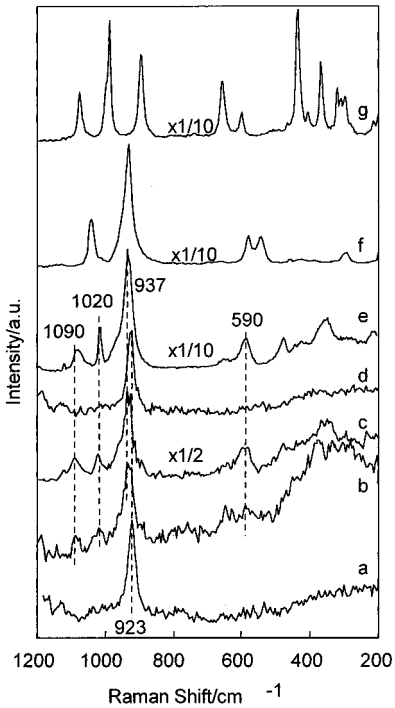

Figure 4. Changes in the Raman spectra upon oxidation. Oxidation state of $(VO)_2P_2O_7$ (C-3) is (a) $x = 0$ (NL = 0, 300 K), (b) $x = 0.047$ (NL = 0.94, 733 K), (c) $x = 0.24$ (NL = 4.9, 773 K), and (d) after the pulse reaction of *n*-butane over oxidized $(VO)_2P_2O_7$. Amount of $(VO)_2P_2O_7$ (C-3): 200 mg (surface V = 1.3×10^{-5} mol). Pulse size of *n*-butane = 6.0×10^{-7} mol. A total of 30 pulses of *n*-butane was introduced at 733 K. Raman spectra of $VOPO_4$: (e) X_1 phase, (f) α-$VOPO_4$, and (g) β-$VOPO_4$.

temperatures at which the amounts of desorbed oxygen correspond to a half monolayer (NL = 0.5) are denoted by $T_{0.5}$ and are shown in Figure 2A. The values of $T_{0.5}$ increased as the oxidation temperature increased and were lower than that for β-$VOPO_4$ ($T_{0.5} = 989$ K, e in Figure 2A). In accordance with the results in Figure 2A, the peak temperature of O_2 desorption became higher as the oxidation temperature increased (Figure 2B).

Changes of the bulk structure of $(VO)_2P_2O_7$ (C-3) upon the controlled oxidation were monitored by XRD. In Figure 3, the XRD patterns of $(VO)_2P_2O_7$ and the oxidized $(VO)_2P_2O_7$ are shown. $(VO)_2P_2O_7$ itself exhibited peaks at $2\theta = 18.4$, 22.8, 28.4, 29.9, and 33.6° (Figure 3, a) which are in good agreement with those in the literature.[23,27] When $(VO)_2P_2O_7$ was oxidized at 713 K for 2 h, the pattern was not changed (Figure 3, b). Upon further oxidation at 733 K, a new broad peak at $2\theta = 21.6°$ appeared (Figure 3, c). This peak became clearer at 753 K (Figure 3, d), and above 773 K, became more intense than that at 22.8° (Figure 3, e and f). The XRD pattern after the oxidation at 823 K (Figure 3, f) was close to that of X_1 phase (Figure 3, g).[4] The XRD pattern of X_1 phase was clearly different from those of α- and β-$VOPO_4$ (Figure 3, h and i).

Changes in the Raman spectra of $(VO)_2P_2O_7$ (C-3) upon the oxidation to controlled extents are given in Figure 4. One main peak was observed at 923 cm^{-1} for $(VO)_2P_2O_7$. Oxidation of $(VO)_2P_2O_7$ at 733 K gave new peaks at 937, 1020, and 1090 cm^{-1}, together with the peak at 923 cm^{-1} (Figure 4, spectrum b). When the sample was oxidized at 773 K, the intensities of the new peaks (937, 1020, and 1090 cm^{-1}) increased (Figure 4, c). These new peaks were not detected for α- and β-$VOPO_4$ (Figure 4, f and g), but are consistent with those of X_1 phase (Figure 4, e).[15] Spectrum d in Figure 4 shows the Raman spectrum obtained after *n*-butane was pulsed 30 times to the sample (0.2 g) which had been used for the experiments shown in Figure 4, b. The size of a pulse was 6.0×10^{-7} mol of *n*-butane. The amount of V atoms exposed to the surface was estimated to be 8.1×10^{-4} mol·g^{-1} from BET surface area (78 m^2·g^{-1}) and the lattice parameters.[23] One pulse thus corresponds to the reduction of 0.052 layer of V^{5+} to V^{4+} (5.2% of V in the monolayer) if 14 electron reduction (corresponding to *n*-butane to MA) of the surface occurred. The peaks due to X_1 phase disappeared completely after the 30 pulses, and the sole peak of $(VO)_2P_2O_7$ recovered. As will be reported in detail in the forthcoming paper, essentially the same changes in the Raman spectra as above were observed by using an in situ Raman cell at 733 K.

The oxidation state of V near the surface was measured by XPS. $(VO)_2P_2O_7$ exhibited two peaks at 524.8 and 517.7 eV due to $V^{4+}2p_{1/2}$ and $V^{4+}2p_{3/2}$, respectively.[15] In the cases of V^{5+} phases such as X_1 phase and β-$VOPO_4$, the peaks appeared at higher binding energies, 526.4 ($V^{5+}2p_{1/2}$) and 518.9 eV ($V^{5+}2p_{3/2}$). For the samples of $(VO)_2P_2O_7$ oxidized at 733 K ($x = 0.047$, NL = 0.94) and 753 K ($x = 0.080$, NL = 1.6), the peaks due to V^{5+} and V^{4+} coexisted.[15] As summarized in Table 1, the ratios of the $2p_{1/2}$ peak intensity, $I_{V^{5+}}/I_{V^{4+}}$, was 0.27 and 0.57 after the oxidation at 733 and 753 K, respectively. The ratios calculated from two models, bulk and surface, are also shown in Table 1. These will be discussed in a later section.

In Figure 5, the conversion of *n*-butane and selectivity to MA during the pulse reaction of *n*-butane with the oxidized $(VO)_2P_2O_7$ (C-3) is shown as a function of the degree of the oxidation, *x*. The data can be compared to the Raman data in Figure 4. Before the reaction, $(VO)_2P_2O_7$ was preoxidized by O_2 at 733 K (NL = 0.94, $x = 0.047$). The first pulse (solid marks in Figure 5) gave the conversion of 80% with the selectivity of 30%. As the number of pulses increased, the

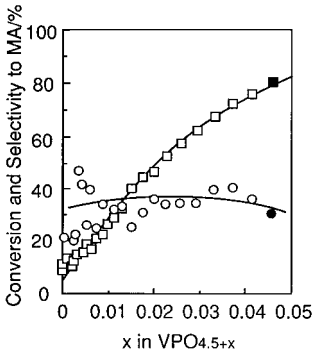

Figure 5. Conversion of *n*-butane and selectivity of maleic anhydride in the pulse reaction as a function of oxidation state of $(VO)_2P_2O_7$. $(VO)_2P_2O_7$ (C-3) was pretreated in an O_2 flow at 733 K for 2 h (x = 0.047, NL = 0.94): (□) conversion, (○) selectivity to MA, catalyst weight; 200 mg. Pulse size of *n*-butane = 6.0×10^{-7} mol. Flow rate of He: 60 mL·min^{-1}. Solid marks show the results of the first pulse.

Table 1. XPS Peak Intensity Ratio of V^{5+} and V^{4+} ($I_{V^{5+}}/I_{V^{4+}}$)

	peak intensity ratio $I_{V^{5+}}/I_{V^{4+}}$			
		calculated		
catalyst	observed	bulk model	surface model	x
$(VO)_2P_2O_7$				
fresh	0	0	0	0.0
oxidized at 733 K	0.27	0.10	0.27	0.047
oxidized at 753 K	0.57	0.19	0.50	0.080
X_1 phase				0.5

conversion decreased, while the selectivity did not change much (30−40%). In the region of low conversions, selectivities were rather scattered, due to the experimental error. When *n*-butane was pulsed to fresh $(VO)_2P_2O_7$ (NL = 0, x = 0), the conversion was low from the first pulse (conversion; 8%, selectivity; 12%) and further decreased to 0% (fourth pulse).

To estimate the oxidation state of $(VO)_2P_2O_7$ during the reaction, a mixture of *n*-butane and O_2 (*n*-butane; 2.6×10^{-7} mol, O_2; 1.3×10^{-6} mol) was pulsed onto the fresh $(VO)_2P_2O_7$ (C-3). The O_2 uptake in the pulse reaction was determined by using the amount of oxygen atoms at the inlet (O_2(inlet)) and that in the products at the outlet (O_2(outlet), CO_2, CO, and MA) as follows: $NL = 4(O_2(\text{inlet}) - O_2(\text{outlet}) - {}^{13}/_2CO_2 - {}^{9}/_2CO - {}^{7}/_2MA)/V_{surf}$, where the sum of O_2 uptake is expressed by NL. V_{surf} is the number of V atom exposed to the surface, estimated from the BET surface area and the lattice parameters.[23] As shown in Figure 6, NL increased with the pulse number and became constant, NL = 0.18, after about 15 pulses.

Figure 7 shows the Fourier transforms of V K-edge EXAFS of α-, β-$VOPO_4$, $(VO)_2P_2O_7$ (C-3), and $VOHPO_4{\cdot}0.5H_2O$ (P-3) measured as standard samples. $(VO)_2P_2O_7$ has a main peak around 1.5−2.2 Å and a weak peak at 3.20 Å (Figure 7, c). $VOHPO_4{\cdot}0.5H_2O$ gives a pattern similar to $(VO)_2P_2O_7$ (peaks at 1.5−2.2 and 3.10 Å) (Figure 7, d). Considering the structures of these compounds,[23,28] the peak around 1.5−2.2 Å is assigned to V═O and V−O distances, and the peak at 3.2 Å corresponds to V−V and V−P distances.[33,34] It should be noted that α- and β-$VOPO_4$ (Figure 7, a and b) showed only one peak at 1.5−1.9 Å, which corresponds to the V−O distance.[18,19]

Figure 8 provides the Fourier transforms of the bulk X_1 phase analyzed by using different Fourier transform regions. Two peaks around 1.58−2.28 and at 3.15 Å were always observed

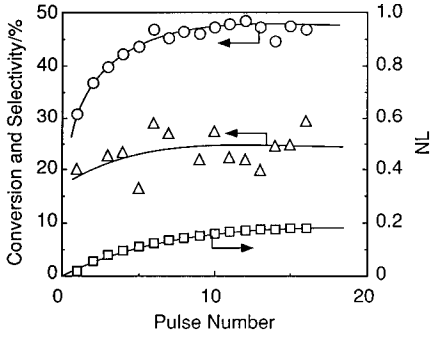

Figure 6. Conversion of *n*-butane, selectivity to maleic anhydride, and change of the number of oxidized surface layers (NL) during the co-pulse reaction of butane−O_2. $(VO)_2P_2O_7$ (C-3) was pretreated in an He flow at 733 K for 2 h (x = 0.0, NL = 0.0): (○) conversion, (▲) selectivity to MA, (□) number of oxidized surface layers; catalyst weight, 200 mg. Pulse size: *n*-butane, 2.6×10^{-7} mol; O_2 1.3×10^{-6} mol. Flow rate of He: 60 mL·min^{-1}.

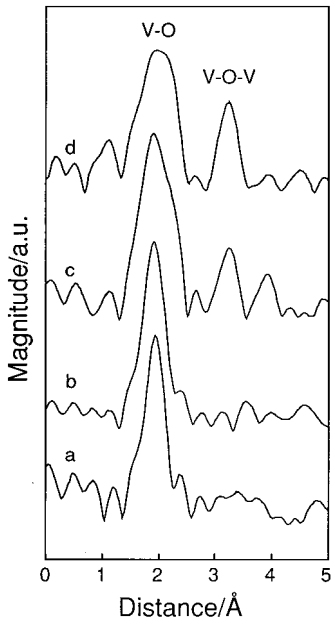

Figure 7. Fourier transform of V K-edge EXAFS of (a) α-$VOPO_4$, (b) β-$VOPO_4$, (c) $(VO)_2P_2O_7$ (C-3), and (d) $VOHPO_4{\cdot}0.5H_2O$.

in these ranges of the Fourier transform. It is noted that the peak positions are similar to those observed for $(VO)_2P_2O_7$ and $VOHPO_4{\cdot}0.5H_2O$.

Transmission electron diffraction (TED) patterns of the bulk $(VO)_2P_2O_7$ (C-4) and X_1 phase are shown in Figure 9, where the bulk X_1 phase was prepared from C-4 having a plate-like structure and was determined to have a single phase by XRD. When the electron beam was incident to $(VO)_2P_2O_7$ along [100], which is vertical to the basal plane, spots were obtained as shown in Figure 9a. The TED image of $(VO)_2P_2O_7$ was the same as that already reported,[35,36] and the cell parameters were determined to be b = 16.53 Å and c = 9.53 Å by using the equation $d = L\lambda/r$, where d is the d spacing, L is the focus length from the sample to the photo film at the observation point in the TED, λ is the wavelength of the electron beam, and r is the distance between observed spots. The values used for the calculation were as follows, $L\lambda$ = 2.12 mm·nm and r for direction b and c were 5.13 and 4.45 mm, respectively. These cell parameters are close to those obtained from the single-

(33) Vlaic, G.; Garmassi, F. *J. Catal.* **1990**, *122*, 312.
(34) Centi, G.; Trifiro, F.; Busca, G.; Ebner, J.; Gleaves, *J. Faraday Discuss. Chem. Soc.* **1989**, *87*, 215.
(35) (a) Bordes, E.; Courtine, P. *J. Catal.* **1979**, *57*, 236. (b) Bordes, E.; Courtine, P. *J. Solid State Chem.* **1984**, *55*, 270.
(36) Torardi, C. C.; Calabrese, J. C. *Inorg. Chem.* **1984**, *23*, 1308.

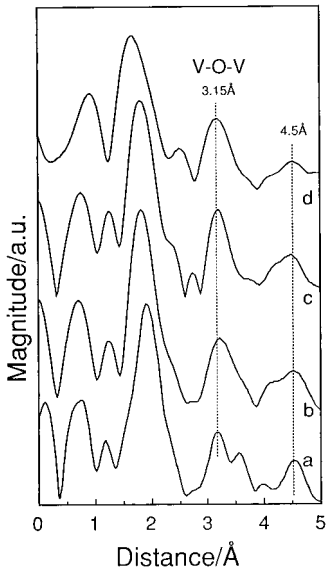

Figure 8. Fourier transform of V K-edge EXAFS of the bulk X_1 phase. V K-edge EXAFS was transformed at FT region of κ = (a) 3.15−13.15, (b) 5.4−13.4, (c) 5.45−15.45, and (d) 7.4−15.4.

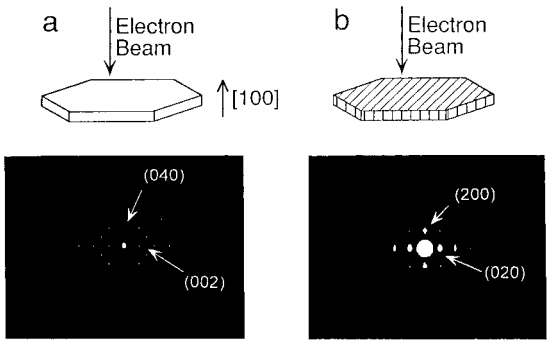

Figure 9. Transmission electron diffraction patterns of (a) $(VO)_2P_2O_7$ (C-4) and (b) X_1 phase derived from $(VO)_2P_2O_7$ (C-4).

crystal XRD.[23] The TED pattern of X_1 phase is shown in Figure 9b. When the electron beam was incident to the X_1 phase along the [100] direction of the parent $(VO)_2P_2O_7$, cell parameters of X_1 phase were determined to be a = 8.22 Å (r = 5.16 mm) and b = 9.40 Å (r = 4.51 mm). Since these axes are vertical to each other and both of them possess mirror symmetry, an orthorhombic unit cell can be suggested for the X_1 phase, and the space group of X_1 phase is considered to be C_{2v}.

Discussion

Changes of the Surface Structure of $(VO)_2P_2O_7$ upon Oxidation and Reduction Treatments. The selective oxidation of *n*-butane over $(VO)_2P_2O_7$ has been considered to proceed via a redox mechanism at the surface layers.[8,13−15] Pepera et al. reported that the number of surface layers involved in the redox processes during the oxidation of *n*-butane is about unity.[13] The reaction between *n*-butane and the oxygen atoms of the catalyst took place only when $(VO)_2P_2O_7$ was oxidized.[13,15] This was confirmed in the present study, as well. When the V^{5+} ions on the surface of the oxidized $(VO)_2P_2O_7$ were reduced back to V^{4+} by the reaction with pulsed *n*-butane, the conversion of *n*-butane decreased to almost 0% (Figure 5). This shows that V^{5+} is necessary for *n*-butane oxidation and the redox cycle between V^{4+} and V^{5+} is involved in the catalytic oxidation. Shimoda et al.[4] reported that the valence of V atom after the steady-state reaction was slightly higher than 4, which is consistent with the above idea. Therefore, the participation of V^{3+} in the redox cycle must not be significant, though it has been suggested to be significant.[1,16,17]

When the catalyst was oxidized by O_2 at 733 K, V^{4+} atoms equivalent in quantity to the monolayer were oxidized to V^{5+} (Figure 1). The location of V^{5+} can be estimated from the XPS data as follows. If the whole bulk of $(VO)_2P_2O_7$ is oxidized uniformly ("bulk-oxidation"), the ratio, V^{5+}/V^{4+}, at the surface should be equal to the bulk V^{5+}/V^{4+} ratio. In this case, the ratios of the surface V^{5+}/V^{4+} ($=I_{V^{5+}}/I_{V^{4+}}$) are calculated to be 0.10 and 0.19 after the oxidation at 733 and 753 K, respectively (Table 1). If $(VO)_2P_2O_7$ is oxidized stepwise from the surface ("surface oxidation"), the V^{5+}/V^{4+} on the top surface becomes infinity at the monolayer oxidation, but the $I_{V^{5+}}/I_{V^{4+}}$ ratios become 0.27 and 0.50 at x = 0.047 (733 K) and x = 0.080 (753 K), respectively, as estimated by considering the escape depth of the photoelectron.[38] This estimation is based on the data of Scofield[39] ($\sigma_{V^{5+}} \approx \sigma_{V^{4+}} = 6.37$ in units of 13 600 × 10^{-28} m^2) for the photoionization crosssection of V^{5+} and V^{4+}, the mean free paths of the photoelectron (λ)[40] $\lambda_{V^{5+},V^{5+}} = 1.53$ nm, $\lambda_{V^{5+},V^{4+}} = 1.54$ nm, and $\lambda_{V^{4+},V^{4+}} = 1.48$ nm, densities of V^{5+} and V^{4+} ($n_{V^{5+}} = 1.2 \times 10^{-5}$ nm^{-3}, $n_{V^{4+}} = 1.3 \times 10^{-5}$ nm^{-3})[21,23] and the thickness of an ideal V^{5+} phase monolayer (t = 0.41 nm). The XPS data are significantly greater than those expected from the bulk oxidation model and much closer to those of the surface oxidation as shown in Table 1. This result shows that the oxidation occurred at a top few surface layers of $(VO)_2P_2O_7$. This conclusion is consistent with our previous result obtained by using $^{18}O_2$, that is, the oxygen diffusion was limited in a few layers from the surface under the reaction conditions.[14]

The oxidation of $(VO)_2P_2O_7$ (Figure 4, b) brought about new Raman peaks (937, 1020, and 1090 cm^{-1}) which are assigned to X_1 phase (Figure 4, e),[8] but not to α- and β-$VOPO_4$. Since the surface P/V ratio of $(VO)_2P_2O_7$ was about unity as determined by XPS, it is reasonable that the oxidation of $(VO)_2P_2O_7$ produced X_1 phase (bulk P/V ratio is unity). When $(VO)_2P_2O_7$ was oxidized at higher temperatures (Figure 3), the formation of X_1 phase was confirmed by XRD, as well. The Raman peaks of X_1 phase, which was formed near the surface as discussed above, disappeared by the reaction with *n*-butane, and a single peak corresponding to $(VO)_2P_2O_7$ was recovered (Figure 4). This fact suggests that the surface X_1 phase is the active phase for the oxidation of *n*-butane and that a redox cycle between $(VO)_2P_2O_7$ and X_1 phase is involved in the catalytic oxidation.

Structure of Surface-Oxidized Layers. As for the real active phase for $(VO)_2P_2O_7$, Volta et al. claimed from Raman spectroscopy and solid-state NMR[8] that the surface layers are γ- and δ-$VOPO_4$ (this phase is similar to X_1 phase) and these phases have isolated VO_6 octahedra. On the other hand, Matsuura proposed from the powder XRD[21] that β'' phase (equivalent to X_1 phase) contains V−O−V pair sites. The present authors suggested by using EXAFS that the structure of X_1 phase resembles that of $(VO)_2P_2O_7$ which contains V−O−V pair sites.[25]

When $(VO)_2P_2O_7$ was oxidized to the degree equivalent to the oxidation of V^{4+} to V^{5+} on the surface monolayer, the

(37) (a) Contractor, R. M.; Bergna, H. E.; Horowitz, H. S.; Blackstone, C. M.; Malone, B.; Torardi, C. C.; Griffiths, B.; Chowdhry, U.; Slight, A. W. *Catal. Today* **1987**, *1*, 49. (b) Contractor, R. M.; Slight, A. W. *Catal. Today* **1987**, *1*, 587.
(38) Inumaru, K.; Okuhara, T.; Misono, M. *J. Phys. Chem.* **1991**, *95*, 4826.
(39) Scofield, J. H. *J. Electron Spectrosc. Relat. Phenom.* **1976**, *8*, 129.
(40) Penn, D. R. *J. Electron Spectrosc. Relat. Phenom.* **1976**, *9*, 29.

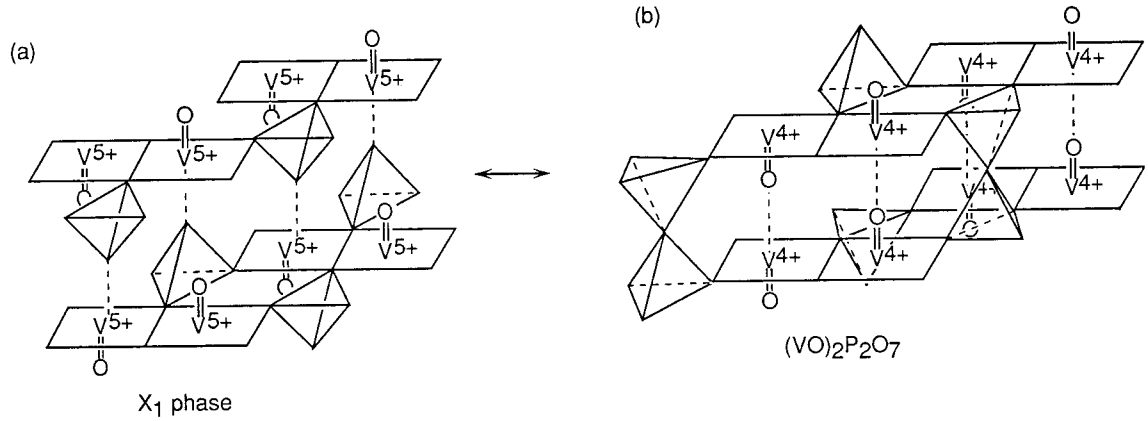

Figure 10. Proposed structure of X_1 phase.

formation of X_1 phase was confirmed by Raman spectroscopy (Figures 3 and 4), while it was hard to detect by XRD. The average number of oxidized surface layers was below unity, showing that the small amount of X_1 phase is present on the surface. This result is consistent with the result of XPS that the oxidation took place only near the surface. X_1 phase is the new phase which was reported by the authors.[4] Matsuura et al.[21] reported the same XRD pattern. A similar phase (δ-$VOPO_4$) showing nearly identical XRD pattern[20] and Raman spectra[8] was reported by Bordes et al. and Volta et al., yet the structure has not been determined.

According to the amount of O_2 uptake, the fraction of X_1 phase was only about $^1/_{10}$ that of $(VO)_2P_2O_7$ phase after the oxidation of C-3 at 733 K (Figure 1a), but the intensity of the Raman peak of X_1 phase was almost comparable to that of $(VO)_2P_2O_7$ (Figure 4a,b). This is most likely due to the difference in the sensitivity that X_1 phase is about 10 times more sensitive than $(VO)_2P_2O_7$. The different sensitivity observed may be explained by the difference in the intensities of scattering caused by the color of each phase and different mode of the main peak for each phase: $\nu(PO_4)$[8] for X_1 phase and ν(P−O−P)[5] for $(VO)_2P_2O_7$.

The Raman peak at 923 cm^{-1} for $(VO)_2P_2O_7$ (Figure 4, a), has been assigned to P−O−P stretching vibration.[5] Volta and co-workers[8] attributed the peak at 935 cm^{-1} of δ-$VOPO_4$ ($\doteqdot X_1$ phase) to PO_4 symmetric stretching vibration. The decrease in the intensity of 923 cm^{-1} peak (ν(P−O−P) of $(VO)_2P_2O_7$) upon the oxidation (Figure 4) shows the structure change of P_2O_7 groups of $(VO)_2P_2O_7$. The change in the structure will be discussed below in more detail.

EXAFS data in Figures 7 and 8 give additional information about the local structure of X_1 phase. The peak at 3.2 is characteristic of $(VO)_2P_2O_7$ and $VOHPO_4{\cdot}0.5H_2O$ and assignable to the atomic distance of V−V in V−O−V units of edge-sharing VO_6 octahedra. VO_6 octahedra are all isolated in α- and β-$VOPO_4$. The contribution of V−O−P bonds to the peaks at 3.2 Å may be small, because the V−O−P angle of corner sharing VO_6 and PO_4 is more variable than the V−O−V angle in edge-sharing VO_6 dimers, hence decreasing the EXAFS peak intensity. Furthermore, lighter P atoms have a lower back-scattering factor than V atoms. If the 3.2 Å peak is due to V−O−V bonds, the fact that the peak at 3.15 Å was always observed for X_1 phase (Figures 7 and 8), being independent of the range of the square window, strongly supports that X_1 phase has the V−O−V pair sites in the structure, as in the case of $(VO)_2P_2O_7$.

By using $a = 8.22$ Å and $b = 9.40$ Å obtained from TED in Figure 9b and assuming that X_1 phase is rhombohedral, c is determined to be 8.21 Å from the XRD pattern in Figure 3. These values for the size of the V_2O_6 pair site unit of X_1 phase ($a = 8.22$, $b = 9.40$) is slightly smaller than that of $(VO)_2P_2O_7$ ($b/2 = 8.26$, $c = 9.56$). This result is consistent with the EXAFS data; the V−V distance was 3.15 Å in X_1 phase, and 3.20 Å in $(VO)_2P_2O_7$ (Figure 7). This difference is probable if one considers that the valence of V is 5+ in X_1 phase, and as a consequence, V−O bond length would become shorter.[41]

Summarizing the above considerations, the structure of X_1 phase may be schematically illustrated as in Figure 10. X_1 phase has a structure related to $(VO)_2P_2O_7$, containing V−O−V pair sites but not P_2O_7.

Relation between Catalytic Performance and Structure of Surface-Oxidized Layers. If the redox mechanism between $(VO)_2P_2O_7$ and X_1 phase is admitted, the oxidation state of the catalyst must be equilibrated at the state where the oxidation rate of $(VO)_2P_2O_7$ is equal to the reduction rate of X_1 phase. When the mixture of O_2 and *n*-butane was pulsed repeatedly to the fresh $(VO)_2P_2O_7$ (C-3), the oxidation state of $(VO)_2P_2O_7$ gradually increased as the pulse number increased and was equilibrated at NL = 0.18 (Figure 6), which corresponds to the state that about 20% of the surface V^{4+} is oxidized to V^{5+}.

With the reaction between the surface X_1 phase and *n*-butane, the Raman peaks corresponding to X_1 phase (937, 1020, and 1090 cm^{-1}) disappeared (Figure 4), and MA was produced concurrently with the selectivity of about 40% (Figure 5), while the selectivity was extremely low for β-$VOPO_4$ (less than 10%).[15] The selectivity to MA over $(VO)_2P_2O_7$ (C-3) under steady-state catalytic conditions was about 50−60%. Hence the selectivity obtained by the present pulse reaction on oxidized $(VO)_2P_2O_7$ is slightly lower than that under steady-state catalytic conditions. A difference is also observed for the selectivity with β-$VOPO_4$ (∼8% (pulse) vs 20% (under steady-state catalytic conditions). Therefore, the experimental errors in the present mass analysis due to the low detectability of MA and the very small amounts of samples could be the major reason for the differences in the selectivity between the two methods. If these reasons are taken into account, it may be inferred that the surface X_1 phase is the real active phase for the catalytic formation of MA over $(VO)_2P_2O_7$.

Spectroscopic analysis of the X_1 phase revealed that X_1 phase contains a structure similar to that of $(VO)_2P_2O_7$ as illustrated in Figure 10. This similarity of the structure between $(VO)_2P_2O_7$ and X_1 phase probably makes the redox cycle facile. The oxygen of the surface X_1 phase desorbed at temperatures lower than that of β-$VOPO_4$, and the desorption temperature from X_1

(41) Hardcastle, F. D.; Wachs, I. E. *J. Phys. Chem.* **1991**, *95*, 5031.

phase tended to decrease as the oxidation temperature decreased (Figure 2), suggesting that X_1 phase formed only on the surface by oxidation at lower temperature is more reactive, and therefore that the surface redox cycle between $(VO)_2P_2O_7$ and X_1 phase is more facile than the redox of the bulk.

Conclusion

Raman spectroscopy and pulse reaction with *n*-butane revealed that X_1 phase is involved in the redox mechanism on the surface of $(VO)_2P_2O_7$. A structure closely related to $(VO)_2P_2O_7$ is proposed for X_1 phase from EXAFS and TED; both having edge sharing VO_6 pairs. Under the steady-state reaction conditions, about 20% of the surface of $(VO)_2P_2O_7$ is oxidized to V^{5+}, crystalline X_1 phase detectable by XRD not being formed. The redox cycle between the surface X_1 phase and $(VO)_2P_2O_7$ is very probably responsible for the selective formation of MA from *n*-butane.

JA964437B